

# Gold-nanourchin complexed silicon dioxide-probe on gap-fingered interdigitated electrode surface for Parkinson's Disease determination by current–volt measurement

Xiaohong Li<sup>1</sup>, Wei Shi<sup>2</sup>, Wenyan Zhang<sup>1</sup>, Weiyao Chen<sup>1</sup>,  
Dan Cao<sup>3</sup>, Subash CB Gopinath<sup>4,5</sup> , Periasamy Anbu<sup>6</sup> ,  
and Na Liu<sup>1</sup>

## Abstract

Parkinson's disease (PD) is a nervous disorder, affects physical movement, and leads to difficulty in balancing, walking, and coordination. A novel sensor is mandatory to determine PD and monitor the progress of the treatment. Neurofilament light chain (NfL) has been recognized as a good biomarker for PD and also helps to distinguish between PD and atypical PD syndromes. Immunosensor was generated by current–volt measurement on gap-fingered interdigitated electrode with silicon dioxide surface to determine NfL level. To enhance the detection, anti-NfL antibody was complexed with gold-nanourchin and immobilized on the sensing electrode. The current–volt response was gradually increased at the linear detection range from 100 fM to 1 nM. Limit of detection and sensitivity were 100 fM with the signal-to-noise ratio at  $n = 3$  on a linear curve ( $y = 0.081x + 1.593$ ;  $R^2 = 0.9983$ ). Limit of quantification falls at 1 pM and high performance of the sensor was demonstrated by discriminating against other neurodegenerative disease markers, in addition, it was reproducible even in serum-spiked samples. This method of detection system aids to measure the level of NfL and leads to determine the condition with PD.

## Keywords

Neurodegenerative disease, neurofilament light chain, current-volt sensor, immunosensing, gold nanomaterial

Date received: 2 September 2020; accepted: 14 December 2020

Topic Area: Polymer Nanocomposites and Nanostructured Materials

Topic Editor: Leander Tapfer

Associate Editor: Jacqueline Santos

## Introduction

Parkinson's disease (PD) is a progressive brain disorder, occurs in the area of the neurons or nerve cells, and causes problems in the movement.<sup>1,2</sup> A significant loss has been noticed with PD, caused uncomfortable lifestyle and severe health issues. Identifying and diagnosing PD with an ideal biomarker is mandatory to give the proper follow-up treatment.<sup>3</sup> Neurofilament light chain (NfL) is a neuronal cytoplasmic protein, expressed highly in the area of myelinated axons. Researchers found that the level of NfL is increasing in blood and cerebrospinal fluids proportionally and cause neurological disorders, such as traumatic,

<sup>1</sup> Department of Neurology, The First Affiliated Hospital of China Medical University, Shenyang, Liaoning, People's Republic of China

<sup>2</sup> Department of Neurology, Tacheng District People's Hospital, Xinjiang, People's Republic of China

<sup>3</sup> Department of Geriatrics, The Fourth People's Hospital of Shenyang, Shenyang, Liaoning, People's Republic of China

<sup>4</sup> Faculty of Chemical Engineering Technology, Institute of Nano Electronic Engineering, Universiti Malaysia Perlis (UniMAP), Perlis, Malaysia

<sup>5</sup> Institute of Nano Electronic Engineering, Universiti Malaysia Perlis (UniMAP), Kangar, Perlis, Malaysia

<sup>6</sup> Department of Biological Engineering, College of Engineering, Inha University, Incheon, Republic of Korea

## Corresponding author:

Xiaohong Li, Department of Neurology, The First Affiliated Hospital of China Medical University, 155 North Nanjing Street, Shenyang, Liaoning 110001, People's Republic of China.

Email: xiaohongli2020@sina.com



neurogenerative, and PD.<sup>4–6</sup> In particular, it has been proved that the level of NfL is increasing in PD disorder patient and potential alternate biomarkers for neurogenerative diseases. Generating a detection system to quantify NfL level in the cerebrospinal fluid helps to diagnose PD.<sup>7,8</sup> Predominantly, the surface of the sensor plays a crucial role for high-performance detection with a rightly oriented biomolecular immobilization.

Rapid identification, label-free, and quantitative detection of diseases is the primary target in medical healthcare and diagnostic to provide an accurate output. The main focus of modern medical diagnostic is to develop and find new applications with nano-biosensor, applicable to medical benefits. Different nanomaterials, including magnetic nanoparticles, nanofibers, carbon nanotubes, and gold nanoparticles, are being utilized to enhance the detection of biomarkers (protein and DNA) responsible for a specific disease. Probes such as an antibody, aptamer, and DNA have been used with these nanomaterials for generating efficient and specific biosensors. Different tests were displayed with sensors to be perfect in diagnosing the target and yield the results in a lesser span of time. A good sensing surface is needed to quantify the level of NfL at its lower level. An interdigitated electrode (IDE) sensor is a well-established sensor that helps to detect various targets with the probing molecules, such as DNA, RNA, protein, antibody, aptamer, and peptide.<sup>9–11</sup> The configuration of the interdigitated pattern allows two electrodes to be infused. Distance between two electrodes has been minimized to a smaller area, which improves the ion diffusion that results in a good rate capability and power density performance. Spectroscopy and current–volt system are well-established techniques, which help to monitor the liquid changes and solid interface of electrodes formed by biological, physical, and chemical layers during the recognition events.<sup>12–15</sup> The experiments are here demonstrated to quantify the NfL concentration on anti-NfL-modified IDE. The detection of NfL was enhanced by conjugating anti-NfL with gold-nanourchin and immobilized on IDE sensor.

Application of nanomaterials in the field of biosensor showed a fast response and detection of various targeted biomolecules.<sup>16–18</sup> Due to the smaller size and larger surface area, the sensing surface helps to enhance the limit of detection of targeted biomolecule.<sup>19</sup> Among different surface materials, gold is one of the long-standing materials due to its unique optical property and suitability with biomolecular functionalization.<sup>20</sup> Gold nanomaterials have been utilized in two ways in the detection system: one is for surface physical functionalization and the other one is to conjugate with detection or capture biomolecule.<sup>21,22</sup> In this research, anti-NfL was immobilized on the surface of the gold-nanourchin and attached to the sensing surface through chemical modification. This electrode was utilized to measure the NfL level through its interaction with its antibody. This interaction was monitored by observing the changes in the response of current due to the

interaction of NfL and anti-NfL. Further, a gold-nanourchin hybrid was utilized to generate the higher performance sensing.

## Materials and methods

### *Biomolecules and instruments*

(3-Aminopropyl)triethoxysilane (APTES; 99%), 16-mercaptohexadecanoic acid (16-MDA; 99%), and ultra-pure grade phosphate buffer solution (PBS, pH 7.4) were purchased from Sigma-Aldrich (Missouri, USA). Gold-nanourchin (approximately  $1.96 \times 10^{10}$  particles/mL; one optical density (OD); 0.1 mM PBS; size approximately 60 nm) was from Nanocs (New York, USA). Ethanolamine ( $\geq 98\%$ ) was from Fisher Scientific Ltd (Loughborough, UK). Gel-electrophoresis pure NfL antigen and anti-NfL antibody were received from Abcam Research Products (Cambridge, UK). *N*-hydroxysuccinimide (NHS; 98%) and *N*-ethyl-*N'*-(3-dimethylaminopropyl)carbodiimide hydrochloride (EDC;  $\geq 97\%$ ) were purchased from GE Healthcare (Illinois, USA). Field-emission transmission electron microscope (FETEM, Jeol Ltd, Japan), field-emission scanning electron microscope (FESEM, Hitachi Multinational Conglomerate Company, S-4300 SE, Japan), and atomic force microscope (AFM, Nanoscope, Ica, Veeco, New York, USA) were used to analyze the morphology of the gold-nanourchin. A Hawk 3D Optical Surface Profiler (Pemtron Co. Ltd, South Korea) was utilized to monitor IDE surface. Current–volt measurements were conducted by utilizing a Picoammeter (Keithley 6487) with a supply of a linear sweep (0–2 V) at a step of 0.1 V. Positive and negative electrodes were used as a dual probing system with PBS and used as the electrolyte. All reagents are analytical grade and highly pure used without further purification step.

### *Designing pattern on chrome mask*

The current–volt sensor surface pattern was designed using the software “AutoCAD 2013.” The dimensions with the length 7000  $\mu\text{m}$ , width 4000  $\mu\text{m}$ , gap size 75  $\mu\text{m}$ , finger-gap pairs 16 and electrode size 100  $\mu\text{m}$ ; electrode thickness 45 nm; and finger length 3500  $\mu\text{m}$  were utilized to generate the pattern on IDE. The desired dimensions were printed on the photomask, pasted on the chrome glass surface, and then fixed with UV exposure for transferring the pattern. The surface of silicon dioxide was layered with an aluminum thin film by placing in the direction opposite of glass and UV light was exposed (10 s). The prepared pattern was transferred on the electrode by performing the developing process (Figure 1(a)).

### *IDE fabrication*

The IDE was prepared using the conventional fabrication of microelectronic process by the following steps.<sup>23,24</sup>

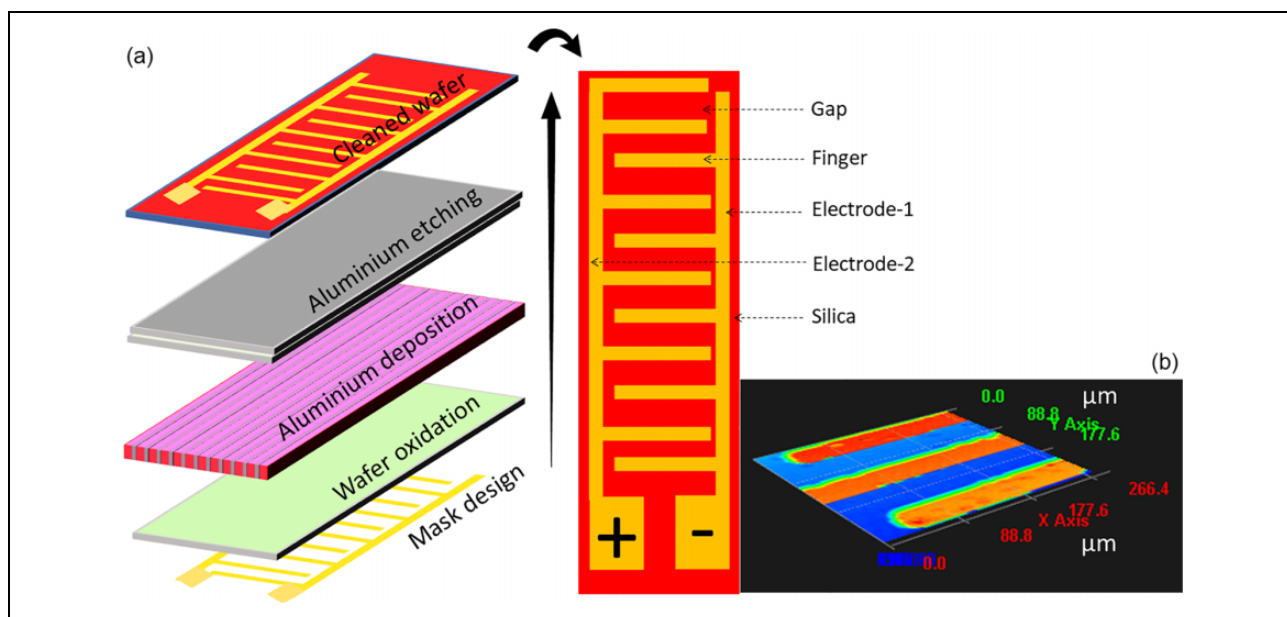


**Figure 1.** (a) Scheme for fabrication steps with IDE. An arrangement on IDE surface is enlarged. (b) The 3D nanoprofiler image of IDE. Gap and finger regions are displayed. IDE: interdigitated electrode.

Initially, the basic IDE with dielectrodes was designed using AutoCAD software and chrome was prepared. (i) Wafer (4 in) containing native oxide was prepared; (ii) inorganic material on the wafer was removed by Piranha and buffered oxide etch solutions; (iii) thick oxide layer with 2800 Å was deposited using the thermal oxidation; (iv) wafer with oxide layer will be scribed quarterly into four for the better handling; (v) aluminum layer with 45 nm was produced using 3 cm long and 0.5 mm diameter using thermal evaporator method with the optimized parameters; (vi) spin-coater (2500 r/min) was used to form a positive photoresist layer; (vii) the surface was soft-baked for 60 s (at 90°C); (viii) chrome mask was arranged with a wafer and UV light was exposed (for 10 s); (ix) unexposed area was removed by RD6 developer; (x) the prepared surface was hard-baked for 120 s (at 90°C); (xi) desired area was removed by aqua regia; and (xii) the produced surface was washed by acetone. The prepared wafer with IDE design at multiple numbers was cut and stored in the desiccator until further use. Before being used, the IDE surface was checked under a microscope and tested by current–voltage system to make sure the fabricated surface was retained.

#### *Preparation of anti-NfL antibody-conjugated gold-nanourchin and UV spectrophotometry*

To conjugate anti-NfL antibody on the gold-nanourchin surface, 1 mL of gold-nanourchin (0.1 OD.; approximately  $0.196 \times 10^{10}$  particles/mL) was added with the mixture of 5 mM 16-MDA and equal ratio of 1-Ethyl-3-(3-dimethylaminopropyl) Carbodiimide (EDC) (200 mM) and N-hydroxysuccinimide (NHS) (50 mM), and stirred this mixture at

room temperature (RT) for 15 min. After that, 200 nM of anti-NfL antibody (approximately  $0.196 \times 10^{10}$  particles/200 nM) diluted in 10 mM PBS (pH 7.4) was added to that solution after removing the unbound molecules by centrifugation ( $10,000 \times g$ ) and kept at RT for 2 h under the condition of stirring. Then, the antibody-conjugated gold-nanourchin was separated by centrifugation as above and washed three times by water. The total concentration of antibodies was measured by nanodrop before and after immobilization. The adsorption of gold-nanourchin before and after immobilization was analyzed using a UV-visible spectrophotometer.

#### *IDE surface functionalization*

Gold-nanourchin-antibody immobilized IDE was formed to quantify the level of NfL antigen. Briefly, 5 μL of APTES was diluted in 30% ethanol, dropped on IDE, and kept at RT for 2 h. And then, the electrode was washed by 30% ethanol followed by 10 mM PBS. Then, the above conjugated 5 μL of gold-nanourchin-antibody was placed on the electrode and kept for 1 h to attach the antibody on IDE. The gold-nanourchin-antibody modified immobilized electrode was utilized to interact with NfL antigen by measuring the current changes upon the interaction.

#### *Detection of NfL antigen on gold-nanourchin-antibody modified surface*

Before detecting NfL antigen, the remaining electrode surface was flooded by ethanolamine to avoid the nonspecific interaction. For that, 1 M of diluted ethanolamine was placed on the gold-nanourchin-antibody modified IDE and

waited for 30 min to mask the uncovered APTES surface.<sup>25</sup> Further, the electrode was washed by PBS, and then, the level of current was noted at this point. Initially, 1 nM of NfL was interacted on the gold-urchin-antibody surface and kept for 10 min. After washing the surface with 10 reaction volumes of PBS, the current level was monitored again. The difference in the current before and after adding NfL was considered as the binding level of NfL antigen with its antibody. Between each step, washings were done and all the experimental conditions were wet, unless otherwise stated.

### *Limit of detection and limit of quantification with NfL interaction*

Limit of detection of NfL was calculated by conducting the experiments with the binding affinity of different linear concentrations of NfL antigen with gold-nanourchin-antibody. For that, NfL antigen concentrations from 10 fM until 1 nM were titrated independently by dropping on the gold-urchin-antibody modified IDE surface. The changes of current between before and after an interaction at each concentration were noted.<sup>26,27</sup> The current differences were plotted in an excel sheet and calculated. The limit of NfL detection was the lowest analyte concentration that was distinguished from the blank as  $3\sigma$  [LOD = standard deviation of the baseline +  $3\sigma$ ]. Limit of NfL quantification is the lowest concentration at which the NfL reliably detected at the condition the predefined goals for bias and imprecision are met.<sup>28</sup> All experiments were conducted in triplicates and estimated ( $n = 3$ ). Blank solution was 10 mM PBS (pH 7.4) and used for the measurements and calculation.

### *Selective detection of NfL and reproducibility*

To demonstrate the high performance, specific control experiments were conducted independently with the neurodegenerative related markers, namely  $\alpha$ -synuclein,<sup>3</sup> DJ-1,<sup>29</sup> and PINK 1.<sup>30</sup> Control proteins at 1 nM were diluted in PBS and interacted on gold-nanourchin-antibody surfaces for 10 min. After washing the surface, the current changes were registered and compared with the similar 1 nM of concentration of NfL antigen. Similar experiments were performed with 1:100 dilution of serum by spiking  $\alpha$ -synuclein, DJ-1, PINK1, and NfL antigen to get to know the selective detection of NfL antigen in the biological samples.

## **Results and discussion**

This research was mainly focused to diagnose the PD with a suitable biomarker using IDE sensor (Figure 1(b)). NfL antigen for determining PD has been proved as one of the good biomarkers and found to be at higher level in PD patient. Effective surface functionalization on the sensor plays a

crucial role in the detection of the desired target. In particular, higher number of probe immobilization on the sensing surface leads to lowering the limit of detection of the target. Different chemical and physical modifications have been utilized to attach a higher biomolecule on the sensing surfaces. Recently, the nanoparticle is getting a greater attraction for the process of surface functionalization. In the current work, gold-nanourchin was utilized to immobilize more numbers of anti-NfL antibodies on IDE using the APTES linker (Figure 2(a)). Before immobilizing the gold-nanourchin-antibody complex on the above surface, the conjugation process of antibody (Figure 2(b)) on the gold-nanourchin was confirmed by UV-Vis spectrometer. The conjugation process involves 16-MDA and has ended with COOH (carboxyl) and SH (thiol) groups. It is widely known that SH has affinity to the gold surface, whereas COOH reacts with amine ( $\text{NH}_2$ ) group, and in the current study, COOH reacts with  $\text{NH}_2$  group on the anti-NfL antibody. EDC helps to conjugate NHS with COOH and forms a stable NHS ester.<sup>31</sup> As shown in Figure 2(c), gold-nanourchin exhibits a maximum peak absorbance of around 520 nm, and the peak was shifted after complexing the antibodies on gold-nanourchin. It clearly shows that the antibody-conjugated gold-nanourchin produces a redshift under the UV-Vis spectrometer scanning. This result attests to the attachment of antibodies on the surface of the gold-nanourchin. This conjugation was utilized to determine the level of NfL antigen on IDE surface. The uniform appearance of IDE surface was confirmed under 3D nanop profiler and clear gap, and finger regions were observed (Figure 1(b)).

### *Surface morphology: Nanoscale imaging*

The intactness of the gold-nanourchin was confirmed by three different high-resolution microscopies (FESEM, FETEM, and AFM). FESEM analyses were performed at  $\times 60$  k and  $\times 150$  k; the obtained images have displayed the uniformly structured and sized gold-nanourchin (Figure 3(a) and (b)). By observing the images, possibly, an organosilane core shell containing anti-NfL antibody has been formed. The measured size of gold-nanourchin was at approximately 60 nm. Similarly, FETEM analyses were done at  $\times 150$  k and  $\times 300$  k high-resolution scales and supported the size of gold-nanourchin to be approximately 60 nm, which displays the size and shape distribution of gold-nanourchin (Figure 3(c) and (d)). Further support was rendered by AFM analysis and the result shows the intact shape and structure of gold-nanourchin (Figure 3(e) and (f)).

### *Biomolecular immobilization on IDE surface*

To determine NfL antigen, gold-nanourchin-antibody conjugation was followed as the probe on IDE. Figure 4(a) shows the immobilization process of gold-nanourchin-antibody on APTES-modified IDE surface. As displayed in the figure, bare surface shows the current level as  $5.0 \times 10^{-7}$  A, after

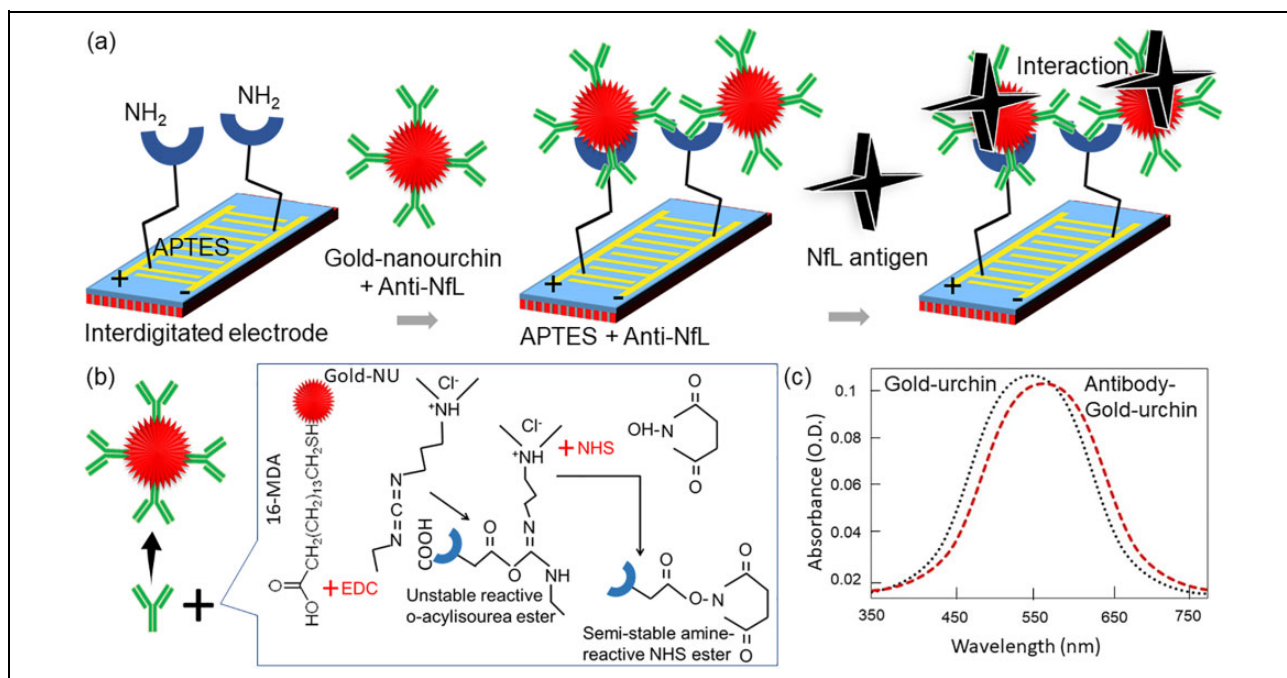


**Figure 2.** (a) Scheme for surface functionalization and detection of NfL on gold-nanourchin-antibody modified IDE. Immobilization process using APTES linker and detected by NfL. (b) Gold-nanourchin conjugation process with antibody. Gold-nanourchin was initially attached with 16-MDA, then activated by EDC and NHC followed by antibody was reacted. (c) UV-Vis spectrometry analysis. Spectrum before and after the antibody attachment on gold-nanourchin is shown. After antibody immobilization can observe from the clear shift of the spectrum. IDE: interdigitated electrode; NfL: neurofilament light chain; EDC: *N*-ethyl-*N'*-(3-dimethylaminopropyl)carbodiimide hydrochloride; 16-MDA: 16-mercaptohexadecanoic acid; APTES: (3-aminopropyl)triethoxysilane.

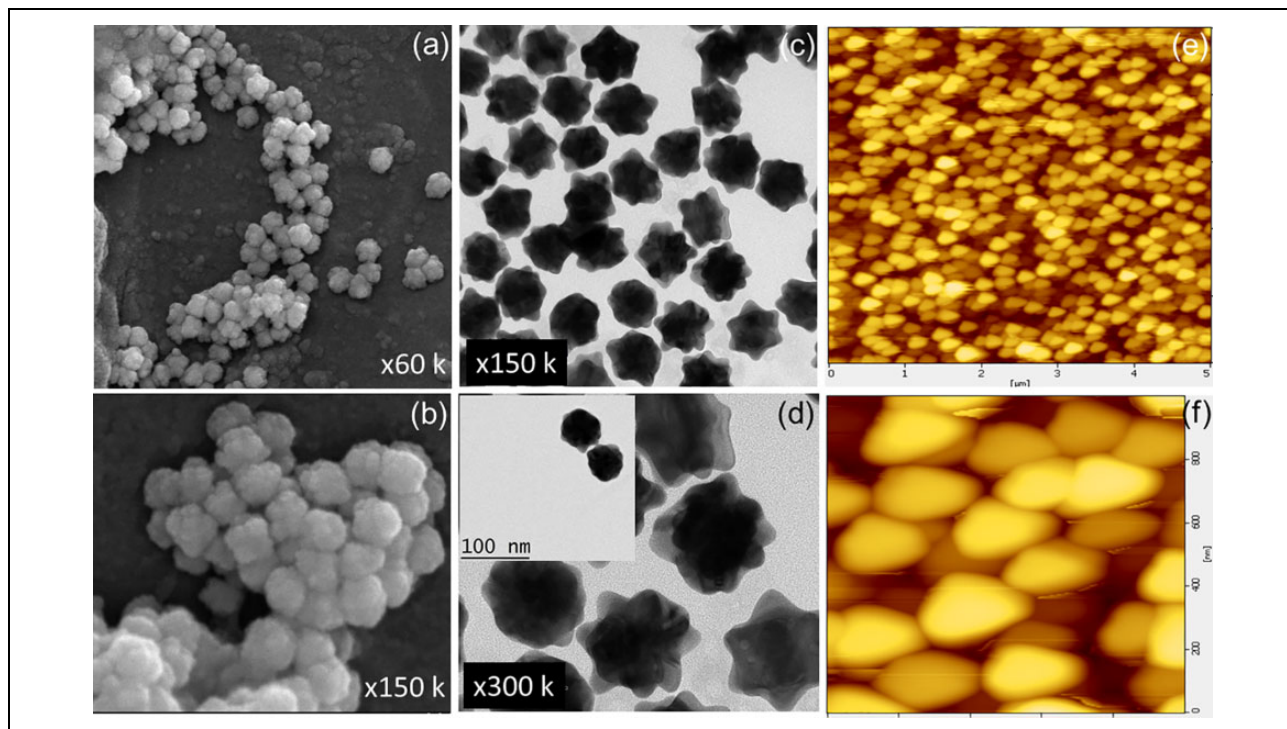


**Figure 3.** Image of gold-nanourchin. (a) FESEM image at  $\times 60$  k. (b) FESEM image at  $\times 150$  k. (c) TEM image at  $\times 150$  k. (d) TEM image at  $\times 300$  k. Figure inset is as-received gold-nanourchin. (e) AFM image with lower magnification (at 5  $\mu\text{m}$ ). (f) AFM image with higher magnification (at 1  $\mu\text{m}$ ). FESEM: field-emission scanning electron microscope; TEM: transmission electron microscope; AFM: atomic force microscope.

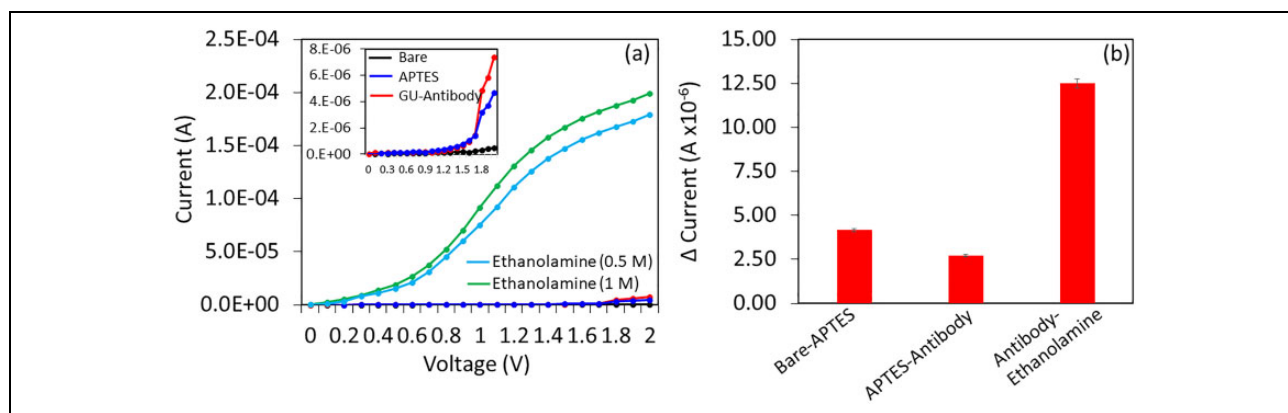


**Figure 4.** Immobilization process of antibody-conjugated gold-nanourchin on the IDE. (a) Current changes after immobilized gold nano-urchin-antibody on the APTES surface. Figure inset is the enlarged graph. Blocking steps were tested by 0.5 and 1 M ethanolamine. (b) Difference in current changes after biomolecular immobilization. IDE: interdigitated electrode; APTES: (3-aminopropyl)triethoxysilane.

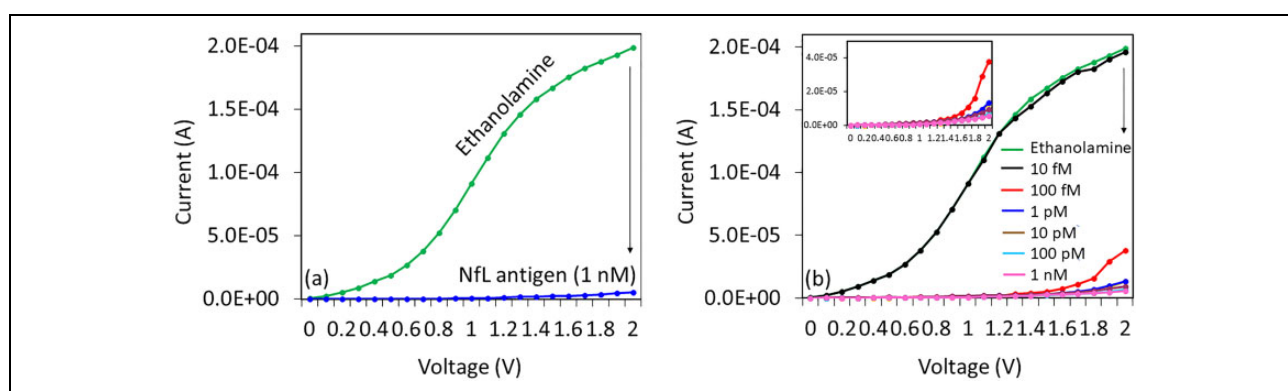


**Figure 5.** (a) Detection of NfL antigen by gold-nanourchin-antibody conjugation. A clear difference in current changes was noted after adding 1 nM of NfL antigen. (b) Different concentrations of NfL antigen interaction with anti-NfL antibody. NfL antigen concentrations from 10 fM to 1 nM were interacted individually on antibody-modified surfaces and the current changes were noted. NfL: neurofilament light chain.

introduced APTES, the current level was increased to  $4.67 \times 10^{-6}$  A. Then, upon adding gold-nanourchin-antibody complex, the current level was increased to  $7.38 \times 10^{-6}$  A and the difference in current was noticed as  $2.71 \times 10^{-6}$  A. The alterations in current confirm the binding of gold-nanourchin-antibody on the chemically modified surface, APTES (Figure 4(b)). These changes in current may happen in two ways: one is due to the interaction of gold-nanourchin with APTES surface and the other possibility is the binding of antibody on APTES surface.<sup>32,33</sup> This immobilization process enhanced the numbers of anti-NfL antibody binding on the surface of IDE surface, which increases the chance for enhancing the NfL antigen detection.

#### Detection of NfL by gold-nanourchin-antibody complex

Before going for the detection of NfL, the ethanolamine was flooded on the surface as the blocking agent to cover

excess space after attaching the antibody. Based on the obtained results in Figure 4(b), 0.5 M ethanolamine was not able to completely cover the free surface on the sensor, however, 1 M ethanolamine was able to perform well. As shown in Figure 5(a), the current level was further increased to  $1.99 \times 10^{-4}$  A after adding the ethanolamine. And then, upon 1 nM of NfL antigen was interacted, the current level decreased to  $3.79 \times 10^{-6}$  A. This drastic current change confirms the interaction of NfL antigen with the immobilized antibody. Moreover, this higher current change was noted due to the binding of higher NfL molecules in higher number on the immobilized anti-NfL. When the antibody was complexed with gold-nanourchin, several antibodies can bind on a single gold-nanourchin, which leads to a higher population of antibodies that can immobilize on IDE surface. Ultimately, this surface can attract higher numbers of NfL antigen, which increases the flow of the current. Based on size analysis, the gold-nanourchin has  $58 \pm 5$  nm, and after conjugating with antibody, it

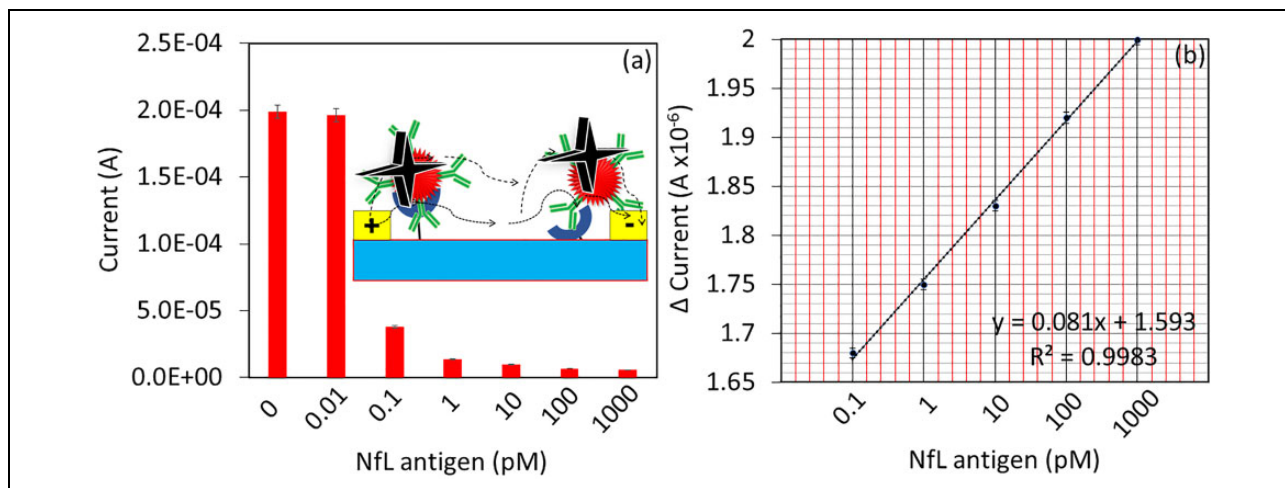


**Figure 6.** (a) Current level with different concentrations of NfL antigen interaction. 200 nM of anti-NfL antibody was interacted. With increasing NfL antigen concentrations, the current changes were gradually decreased. Figure inset is the diagrammatic representation for the dipole moment mechanism on IDE. (b) Linear regression analysis. To calculate the detection limit of NfL, the difference in current changes of NfL interaction with antibody was plotted in an excel file and calculated the detection limit in the linear range of 100 fM to 1 nM ( $n = 3$ ). NfL: neurofilament light chain; IDE: interdigitated electrode.

increased to  $75 \pm 10$  nm. Moreover, it was noticed that the zeta potential of gold-nanourchin was  $-23.5$  mV, and after conjugating with antibody, it shows  $-5$  mV. Gold-nanourchin conjugated antibody has a lower negative charge compared to as-received gold-nanourchin. This result indicated the successful binding of antibody on the surface of the gold-nanourchin.

#### Dose-dependent analysis of NfL: LOD and LOQ

Dose-dependent detection of NfL antigen was performed by titrating NfL concentrations in the linear range from 10 fM to 1 nM and allows to interacting with the immobilized antibody. Figure 5(b) shows the interaction of different concentrations of NfL antigen with its antibody. After the immobilization of gold-nanourchin-antibody complex, ethanolamine blocking was done and it shows the current level as  $1.99 \times 10^{-4}$  A, and then, 10 fM of NfL antigen was added, it did not show any current changes. And then, by enhancing the concentration to 100 fM, the current was decreased to  $3.79 \times 10^{-5}$  A. Further, with the increment in the NfL antigen concentrations to 1 pM, 10 pM, 100 pM, and 1 nM, the current levels were further decreased to  $1.36 \times 10^{-5}$ ,  $9.54 \times 10^{-6}$ ,  $6.76 \times 10^{-6}$ , and  $5.68 \times 10^{-6}$  A (Figure 6(a)). The difference in the current was estimated and the linear range from 100 fM to 1 nM was plotted in an excel sheet. Based on these results, the limit of detection and sensitivity were 100 fM on a linear regression curve ( $y = 0.081x + 1.593$ ;  $R^2 = 0.9983$ ), and the limit of quantification (LOQ) falls with 1 pM with signal-to-noise ratio at  $n = 3$  (Figure 6(b)). The attainments of linear range from 100 fM to 1 nM indicate that the saturation point is not at low nanomolar concentrations.

#### Control experiments: Selectivity and reproducibility on NfL antigen detection

Control experiments were performed with three neurogenerative biomarkers, namely  $\alpha$ -synuclein, DJ-1, and PINK 1 to confirm the specific detection of NfL antigen. For this selective detection, these proteins with the concentration at 1 nM were interacted independently on the gold-nanourchin-antibody immobilized IDE, and then, the current levels were monitored. As shown in Figure 7(a), control proteins do not show the significant current changes compared with the selective detection of NfL antigen on gold-nanourchin-antibody modified surface. Moreover, NfL antigen was spiked in the diluted serum and did not affect the detection, indicating selective detection of NfL antigen in the biological samples (Figure 7(a)). Further, to evaluate the reproducibility of the surface chemical and biological modifications, five different devices were tested and averaged. The obtained results show the reliability of IDE surface for chemical and biological modifications (Figure 7(b)). The stability and the operational lifetime of the fabricated sensing surface can be extended for 3 months under proper storage at desiccator. However, by immobilizing the biomolecule, the surface activity was noticed to be lost approximately 25% after 3 weeks and a further sharp reduction in a few days. However, the biosensor is shown here displaying the disadvantages, such as short-circuit with the gaps at nanoscale levels. In addition, the current-sensing surface is more suitable for oxide materials with appropriate chemical surface functionalization.

The primary advantage of using gold-nanourchin is in this study to create high-performance IDE sensor. The presence of gold-nanourchin on the surface enhances the

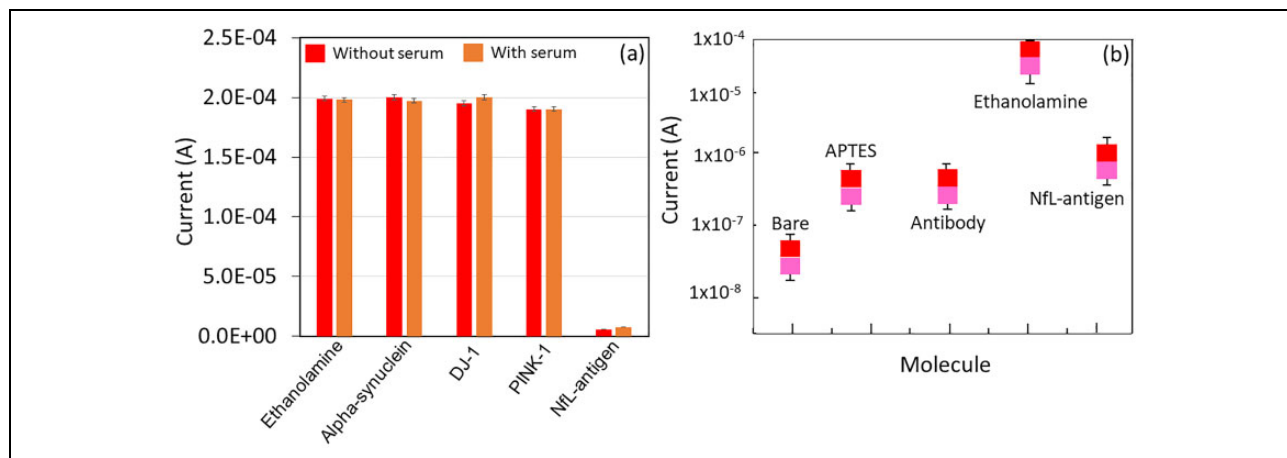


**Figure 7.** (a) Selective detection of NfL. Control proteins namely alpha-synuclein, DJ-1 and PINK I were interacted on anti-NfL antibody modified IDE surface and the current levels were noted. Control proteins did not show the significant changes in current compared with the specific NfL antigen. (b) Reproducibility analysis. Averaged values ( $n = 5$ ) for different surface chemical and biological modifications. NfL: neurofilament light chain; IDE: interdigitated electrode.

**Table 1.** Comparison among currently available sensors for Parkinson's disease.

Sensor	Sensitivity	Linear range	Reference
Electrochemical	5.21 ng/L	1–50 $\mu$ g/L	Özgür et al. <sup>1</sup>
4 Plex A assay	0.104 pg/mL	—	Korley et al. <sup>34</sup>
Immunomagnetic reduction assay	0.18 fg/mL	0.18–1000 pg/mL	Liu et al. <sup>35</sup>
Single molecule array	0.32 pg/mL	0–2000 pg/mL	Gattringer et al. <sup>36</sup>
Electrochemical assay	100 fM	10 fM–1 nM	This work

surface area with the ultimate aim to capture and interact with biomolecules (anti-NfL antibody and NfL) at higher numbers. Further, gold-nanourchin aids to immobilize the probe molecules at proper orientation and alignment. The output of this sensor shows a better performance compared to other currently available immunosensors (Table 1).

## Conclusion

An approach for diagnosing PD with a relevant biomarker is necessary to provide the proper medication and a healthy lifestyle to the affected patient. This study was focused on diagnosing PD with NfL antigen, which was found as a good biomarker. Anti-NfL antibody immobilized interdigitated sensor was used to detect and quantify the NfL level. Further, to enhance the NfL detection, antibody was complexed on the surface of the gold-nanourchin and immobilized on the electrode. The current responses were found to increase when increasing the concentrations of NfL antigen, and limit of detection and LOQ were found as 100 fM. The sensitivity falls at 100 fM and the high performance was proved by the higher selectivity and reproducibility in the presence of serum, indicating the selective detection of NfL antigen. This surface functionalization helps to diagnose PD efficiently and helps for treatment purposes.



## Declaration of conflicting interests

The author(s) declared no potential conflicts of interest with respect to the research, authorship, and/or publication of this article.

## Funding

The author(s) received no financial support for the research, authorship, and/or publication of this article.

## ORCID iD

Subash CB Gopinath  <https://orcid.org/0000-0002-8347-4687>  
Periasamy Anbu  <https://orcid.org/0000-0003-4519-5254>

## References

- Özgür E, Uzunçakmak Uyanık H, Şenel S, et al. Immunoaffinity biosensor for neurofilament light chain detection and its use in Parkinson's diagnosis. *Mater Sci Eng B Solid-State Mater Adv Technol* 2020; 256: 114545.
- Sun K, Xia N, Zhao L, et al. Aptasensors for the selective detection of alpha-synuclein oligomer by colorimetry, surface plasmon resonance and electrochemical impedance spectroscopy. *Sensors Actuators, B Chem* 2017; 245: 87–94.
- Zhang R, Wang S, Huang X, et al. Gold-nanourchin seeded single-walled carbon nanotube on voltammetry sensor for diagnosing neurodegenerative Parkinson's disease. *Anal Chim Acta* 2020; 1094: 142–150.

4. Lin YS, Lee WJ, Wang SJ, et al. Levels of plasma neurofilament light chain and cognitive function in patients with Alzheimer or Parkinson disease. *Sci Rep* 2018; 8: 17368.
5. Rojas JC, Karydas A, Bang J, et al. Plasma neurofilament light chain predicts progression in progressive supranuclear palsy. *Ann Clin Transl Neurol* 2016; 3(3): 216–225.
6. Gaetani L, Blennow K, Calabresi P, et al. Neurofilament light chain as a biomarker in neurological disorders. *J Neurol Neurosurg Psychiatr* 2019; 90: 870–881.
7. Constantinescu R, Rosengren L, Johnels B, et al. Consecutive analyses of cerebrospinal fluid axonal and glial markers in Parkinson's disease and atypical parkinsonian disorders. *Park Relat Disord* 2010; 16(2): 142–145.
8. Hall S, Öhrfelt A, Constantinescu R, et al. Accuracy of a panel of 5 cerebrospinal fluid biomarkers in the differential diagnosis of patients with dementia and/or Parkinsonian disorders. *Arch Neurol* 2012; 69(11): 1–8.
9. Liang T, Qu Q, Chang Y, et al. Diagnosing ovarian cancer by identifying SCC-antigen on a multiwalled carbon nanotube-modified dielectrode sensor. *Biotechnol Appl Biochem* 2019; 66: 939–944.
10. Gopinath SCB, Awazu K, Fujimaki M, et al. Monitoring biological interactions using perforated evanescent-field-coupled waveguide-mode nanobiosensors. *Nucleic Acids Symp Ser (Oxf)* 2009; (53): 93–94.
11. Ong CC, Gopinath SCB, Rebecca LWX, et al. Diagnosing human blood clotting deficiency. *Int J Biol Macromol* 2018; 116: 765–773.
12. Brosel-Oliu S, Galyamin D, Abramova N, et al. Impedimetric label-free sensor for specific bacteria endotoxin detection by surface charge registration. *Electrochim Acta* 2017; 243(2017): 142–151.
13. Wang Y, Guo Y, Lu J, et al. Nanodetection of head and neck cancer on titanium oxide sensing surface. *Nanoscale Res Lett* 2020; 15(1): 33.
14. Lu B, Liu L, Wang J, et al. Detection of microRNA-335-5p on an interdigitated electrode surface for determination of the severity of abdominal aortic aneurysms. *Nanoscale Res Lett* 2020; 15: 105.
15. Zhang J and Gopinath SCB. Quantification of cortisol for the medical diagnosis of multiple pregnancy-related diseases. *3 Biotech* 2020; 10(2): 35.
16. Bonanni A, Fernández-Cuesta I, Borrísé X, et al. DNA hybridization detection by electrochemical impedance spectroscopy using interdigitated gold nanoelectrodes. *Microchim Acta* 2010; 170(3): 275–281.
17. Gopinath SCB, Lakshmpriya T, and Awazu K. Colorimetric detection of controlled assembly and disassembly of aptamers on unmodified gold nanoparticles. *Biosens Bioelectron* 2014; 51: 115–123.
18. Miranda OR, Li X, Garcia-Gonzalez L, et al. Colorimetric bacteria sensing using a supramolecular enzyme-nanoparticle biosensor. *J Am Chem Soc* 2011; 133(25): 9650–9653.
19. Sondhi P, Maruf MHU, and Stine KJ. Nanomaterials for biosensing lipopolysaccharide. *Biosensors* 2020; 10(1): 1–28.
20. Letchumanan I, Gopinath SCB, Md Arshad MK, et al. Gold nano-urchin integrated label-free amperometric aptasensing human blood clotting factor IX: a prognosticative approach for “Royal disease.” *Biosens Bioelectron* 2019; 131(February): 128–135.
21. Bao X, Huo G, Li L, et al. Coordinated dispersion and aggregation of gold nanorod in aptamer-mediated gestational hypertension analysis. *J Anal Methods Chem* 2019; 2019: 5676159.
22. Ali ME, Hashim U, Mustafa S, et al. Gold nanoparticle sensor for the visual detection of pork adulteration in meatball formulation. *J Nanomater* 2012; 2012: 1–7.
23. Ramanathan S, Gopinath SCB, Md Arshad MK, et al. Multidimensional (0D-3D) nanostructures for lung cancer biomarker analysis: comprehensive assessment on current diagnostics. *Biosens Bioelectron* 2019; 141(June): 111434.
24. Letchumanan I, Md Arshad MK, Gopinath SCB, et al. Comparative analysis on dielectric gold and aluminium triangular junctions: impact of ionic strength and background electrolyte by pH variations. *Sci Rep* 2020; 10: 6783.
25. Dalila NR, Arshad MKM, Gopinath SCB, et al. Molybdenum disulfide—gold nanoparticle nanocomposite in field-effect transistor back-gate for enhanced C-reactive protein detection. *Microchim Acta* 2020; 187(11): 588.
26. Letchumanan I, Gopinath SCB, and Arshad MKM. Divalent ion-induced aggregation of gold nanoparticles for voltammetry immunosensing: comparison of transducer signals in an assay for the squamous cell carcinoma antigen. *Microchim Acta* 2020; 187: 128.
27. Hong X, Hong X, Zhao H, et al. Improved immunoassay for Insulin-like Growth Factor 1 detection by aminated silica nanoparticle in ELISA. *Process Biochem* 2020; 91: 282–287.
28. Armbruster DA and Pry T. Limit of blank, limit of detection and limit of quantitation. *Clin Biochem Rev* 2008; 29(Suppl 1): 49–52.
29. Abou-Sleiman PM, Healy DG, Quinn N, et al. The role of pathogenic DJ-1 mutations in Parkinson's disease. *Ann Neurol* 2003; 54: 283–286.
30. Pickrell AM and Youle RJ. The roles of PINK1, Parkin, and mitochondrial fidelity in Parkinson's disease. *Neuron* 2015; 85: 257–273.
31. Welch NG, Scoble JA, Muir BW, et al. Orientation and characterization of immobilized antibodies for improved immunoassays (review). *Biointerphases* 2017; 12(2): 02D301.
32. Vashist SK, Marion Schneider E, Lam E, et al. One-step antibody immobilization-based rapid and highly-sensitive sandwich ELISA procedure for potential in vitro diagnostics. *Sci Rep* 2014; 4: 4407.
33. Chen H, Zhao L, Chen D, et al. Stabilization of gold nanoparticles on glass surface with polydopamine thin film for

- reliable LSPR sensing. *J Colloid Interface Sci* 2015; 460: 258–263.
34. Korley FK, Yue JK, Wilson DH, et al. Performance evaluation of a multiplex assay for simultaneous detection of four clinically relevant traumatic brain injury biomarkers. *J Neurotrauma* 2019; 36: 182–187.
35. Liu HC, Lin WC, Chiu MJ, et al. Development of an assay of plasma neurofilament light chain utilizing immunomagnetic reduction technology. *PLoS One* 2020; 15(6): e0234519.
36. Gattringer T, Pinter D, Enzinger C, et al. Serum neurofilament light is sensitive to active cerebral small vessel disease. *Neurology* 2017; 89(20): 2108–2114.